Novel Poly(*p*-phenylene vinylene) Derivatives with Oligo(ethylene oxide) Side Chains: Synthesis and Pattern Formation

Berthold Winkler, Liming Dai,* and Albert W.-H. Mau*

CSIRO Molecular Science, Bag 10, Clayton South, Victoria 3169, Australia

Received August 18, 1998. Revised Manuscript Received November 13, 1998

We used a Gilch or sulfonium precursor route to prepare 2,5-substituted poly(*p*-phenylenevinylene) (PPV) derivatives with methoxy-terminated oligo(ethylene oxide) side chains (EO_m−PPV, $EO_m = CH_3O(CH_2CH_2O)_m$ and $m = 1-3$). The intermediate and final products were characterized by UV−vis, FTIR, and NMR spectroscopy. A bathochromic shift from $\lambda_{max} = 476$ nm ($m = 1$) to $\lambda_{max} = 511$ nm ($m = 3$) and a constant optical band gap between 2.13 and 2.14 eV were observed in the UV−vis spectra for the resultant conjugated polymers with different side chain lengths. The red EO_m−PPV showed similar photo- and electroemissions at ca. 600 nm. Single layer LEDs with the structure ITO/EO_m−PPVs/Al showed turn-on voltages at ca. 7 V. Pattern formation was achieved by patterned plasma polymerization of acetic acid onto, for example, perfluorinated ethylene−propylene copolymer (FEP) films, followed by selective adsorption of EO_3−PPV from chloroform solutions.

Introduction

Conjugated polymers have attracted much interest for potential applications in optoelectronic devices due to their exceptional electronic and photonic properties.[1,2] Poly(*p*-phenylene vinylene) (PPV) and its derivatives in particular, have been extensively studied since the first report on a polymer-based light-emitting diode (LED) in 1990 by Burroughes et al.[3] Owing to their relatively high photoluminescence (PL) and electroluminescence (EL) quantum efficiencies[4] and good color tunability through molecular engineering, PPVs are the most attractive materials for EL applications. Upon application of an electrical voltage to an EL device, electrons from the low-work-function cathode (e.g., Al) are injected into the lowest unoccupied molecular orbital (LUMO) of the organic semiconductor, leading to the formation of negatively charged polarons, whereas holes from the high -work-function anode (e.g., indium tin oxide, ITO) are injected into the highest occupied molecular orbital (HOMO), producing positively charged polarons. Emission from the active layer results from the formation of a singlet exciton which is generated by charge annihilation of the injected holes and electrons. Therefore, the emission wavelength (and hence the color) depends on the energy gap of the organic light-emitting material, coupled with the Stokes shift.

Recently, Heeger and co-workers reported electrochemically driven light-emitting cells (LECs), in which an in situ light-emitting p−n junction was formed by simultaneous p-type and n-type electrochemical doping of electrolyte-containing conjugated polymer chains between two oppositely charged electrodes.[5] While various PPV derivatives substituted with alkoxy, alkyl, aryl, halogen, and alkylsilyl side groups have been used in LEDs,[6] EL polymers with very polar side chains, such as the oligo(ethylene oxide)-grafted PPVs (EO_m−PPV, $EO_m = CH_3O(CH_2CH_2O)_m$ and $m = 1-3$) reported in this paper, should be very useful for LEC applications because the polar substituents can act as ionic conducting components to facilitate the electrochemical doping processes. Because of the covalent linkages between the oligo(ethylene oxide) side chains and the conjugated backbone, the phase separation problem often associated with those more conventional LEC devices[5,7] based on the mixture of polymeric ion conductors [e.g., poly(ethylene oxide), PEO] and π-conjugated polymers could be minimized. This has been previously demonstrated for LECs made from poly[9,9-bis(3,6-dioxaheptyl)fluorene-2,7-diyl].[7]

(1) Sheats, J. R.; Antoniadis, H.; Hueschen, M.; Leonard, W.; Miller, J.; Moon, R.; Roitman, D.; Stocking, A. *Science* 1996, *273*, 884.

(2) Proceedings of International Conference on Science and Technology of Synthetic Metals − ICSM'96, Snowbird (USA), *Synth. Met.* **1997**, *84*−*86*.

(3) Burroughes, J. H.; Bradley, D. D. C.; Brown, A. R.; Marks, R. N.; Mackay, K.; Friend, R. H.; Burn, P. L.; Holmes, A. B. *Nature* **1990**, *347*, 539.

(4) (a) Greenham, N. C.; Samuel, I. D. W.; Hayes, G. R.; Phillips, R. T.; Kessener, Y. A. R. R.; Moratti, S. C.; Holmes, A. B.; Friend, R. H. *Chem. Phys. Lett.* **1995**, *241*, 89. (b) Son, S.; Dodabalapur, A.; Lovinger, A. J.; Galvin, M. E. *Science* **1995**, *269*, 376.

(5) (a) Pei, Q.; Yu, G.; Zhang, C.; Yang, Y.; Heeger, A. J. *Science* **1995**, *269*, 1086. (b) Pei, Q.; Yang, Y.; Yu, G.; Zhang, C.; Heeger, A. J. *J. Am. Chem. Soc.* **1996**, *118*, 3922.

(6) (a) Andersson, M. R.; Yu, G.; Heeger, A. J. *Synth. Met.* 1997, *85*, 1275. (b) Shim, H.-K.; Jang, M.-S.; Hwang, D.-H. *Macromol. Chem.* **1997**, *198*, 353. (c) Winkler, B.; Tasch, S.; Zojer, E.; Ungerank, M.; Leising, G.; Stelzer, F. *Synth. Met.* **1996**, *83*, 177. (d) Wan, W. C.; Antoniadis, H.; Choong, V. E.; Razafitrimo, H.; Gao, Y.; Feld, W. A.; Hsieh, B R. *Macromolecules* **1997**, *30*, 6567. (e) Hsieh, B. R.; Antoniadis, H.; Bland, D. C.; Feld, W. A. *Adv. Mater.* **1995**, *7*, 36. (f) Gurge, R. M.; Sarker, A. M.; Lahti, P. M.; Hu, B.; Karasz, F. E. *Macromolecules* **1997**, *30*, 8286. (g) Hochfilzer, C.; Tasch, S.; Winkler, B.; Huslage, J.; Leising, G. *Synth. Met.* **1997**, *85*, 1271. (h) Winkler, B.; Meghdadi, F.; Tasch, S.; Müllner, R., Resel, R.; Saf, R.; Leising, G.; Stelzer, F. *Opt. Mater.* **1998**, *9*, 159.

(7) (a) Yang, Y.; Pei, Q. *J. Appl. Phys.* **1997**, *81*, 3294. (b) Pei, Q.; Yang, Y. *J. Am. Chem. Soc.* **1996**, *118*, 7416.

10.1021/cm980570m CCC: $18.00
Published on Web 02/06/1999

Recent developments in polymeric EL studies have indicated the possibility of using LEDs and/or LECs for color displays.[8] Pattern formation, and hence patterned emission, is important for such applications. Although a few approaches have been devised for patterning certain conjugated polymers,[9] a general patterning method applicable to all conjugated polymers is still not in sight and, as far as we are aware, pattern formation of oligo(ethylene oxide)-grafted conjugated polymers has not been reported. On the basis of our previous work on microstructuring of polypyrrole and polyaniline by selective electropolymerization of the corresponding monomers onto plasma patterned surfaces,[10] we have developed a method to produce patterns of EO_3−PPV by selective adsorption of its polar side chains onto, for example, perfluorinated ethylene−propylene copolymer (FEP) films prepatterned by hydrophilic plasma polymers (e.g., acetic acid plasma). The EO_3−PPV patterns thus formed show fluorescence emission, which enables visualization of the conjugated polymer regions under a fluorescence microscope.

While this work was in progress, we noted that the synthesis of EO_3−PPV via the Gilch route was briefly described in conference papers.[11] To synthesize EO_m−PPVs with a wide range of *m* for elucidating possible effects of the side chain length on the optoelectronic properties, we have used both the Gilch route and sulfonium precursor route in this study.[12] We found that the sulfonium precursor route was particularly effective for making EO_m−PPVs with short side chains ($m < 3$), whereas the Gilch route had to be used for the synthesis of EO_3−PPV. PPVs prepared by both methods are generally known to have relatively high molecular weights, with their conjugated backbones mainly consisting of *trans*-vinylene units. In this paper we report the detailed synthesis and characterization of EO_m−PPVs, along with the fabrication of LED devices and surface patterns from them.

Scheme 1

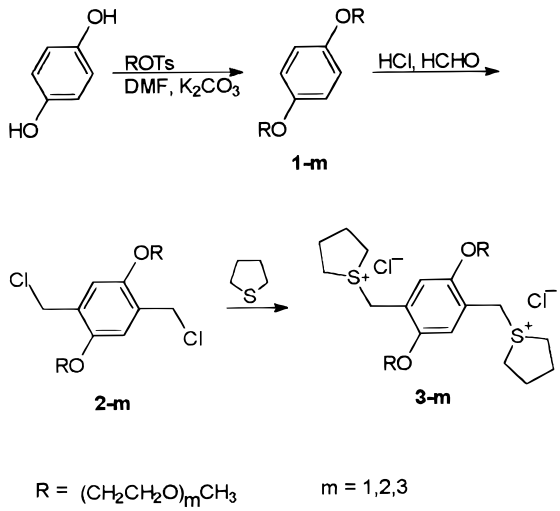

Experimental Section

Characterization. ^1H and ^{13}C nuclear magnetic resonance (NMR) spectra were recorded on a Bruker AC-200 NMR spectrometer. Fourier transform infrared (FTIR) spectra were measured on a Bomem MB-100 FTIR spectrometer using a free-standing film, with samples cast on a KRS-5 crystal or KBr disk, while an atmospheric pressure chemical ionization/electrospray mass spectrometer (MS, Micromass Platform II) was used to confirm the structure of small molecules. Ultraviolet−visible (UV−vis) measurements were made on a Cary 5E UV/VIS/NIR spectrophotometer. PL spectroscopy was performed on a luminescence spectrometer SL 50 from Perkin-Elmer. PL efficiency in CH_3CN was determined with Rhodamine B as reference (λ_{ex} = 370 nm, F = 0.71).[13] Size exclusion chromatography (SEC) was recorded on a Waters Associates SEC system, using THF as the eluent and a low-dispersity polystyrene standard. X-ray photoelectron spectroscopy (XPS) analyses were performed on an AXIS HSi spectrometer by Kratos Analytical with monochromatized Al Kα radiation. Air/liquid contact angles were determined on a Kernco G-II goniometer equipped with a syringe incorporating a reversible plunger driven by a micrometer and using Milli-Q water as test liquid. This instrument allowed the determination of advancing (ACA), sessile (SCA), and receding (RCA) contact angles for the same sample.[14] Typically, three to five measurements were made and their average values were taken as the reported contact angles. EL emissions from the LEDs were measured by an EG&G Model 1460 optical multichannel analyzer, while their diode characteristics were determined using a Hewlett-Packard 6113A DC power supply and a Fluke 45 dual display multimeter. Fluorescence microscopic images of the EO_3−PPV patterned surfaces were recorded on an Olympus IMT2-RFL fluorescence microscope attached to a dichroic mirror unit IMT2-DMB for excitation with blue light. All above measurements were carried out under ambient conditions (20 °C).

Materials. The starting materials for the chemical reactions shown in Schemes 1 and 2 were purchased from Fluka and Aldrich and used as received. Oxaalkyl-*p*-toluenesulfonates were synthesized according to a reported method.[15] All other chemicals were reagent grade and purchased from commercial sources.

1,4-Bis(1,4-dioxapentyl)benzene (1−1). Hydroquinone (4.4 g, 40 mmol) was added to a solution of K_2CO_3 (18.2 g) in DMF (70 mL) and stirred at 60 °C for 15 min under N_2. To the resulting yellow solution was added 3-oxabutyl-*p*-toluene-

(8) (a) Kraft, A.; Grimsdale, A. C.; Holmes, A. B. *Angew. Chem., Int. Ed. Engl.* **1998**, *37*, 402. (b) Dai, L.; Winkler, B.; Huang, S.; Mau, W. A. H. In *Semiconductive Polymers*; American Chemical Society: Washington, DC (in press).

(9) See, for example: (a) Rozsnyai, L. F.; Wrighton, M. S. *J. Am. Chem. Soc.* **1994**, *116*, 5993. (b) Martin, C. R. *Acc. Chem. Res.* **1995**, *28*, 61. (c) Allen, P. C.; Bott, D. C.; Connors, L. M.; Gray, S.; Walker, N. S.; Clemenson, P. I.; Feast, W. J. *Electronic Properties of Conjugated Polymers III*; Kuzmany, H., Mehring, M., Roth, S., Eds.; Springer-Verlag: 1989; p 456. (d) Zenkl, E.; Schimetta, M.; Stelzer, F. *Polymers for Microelectronics*; Thompson, L. F., Willson, C. G., Tagawa, S., Eds.; ACS Symp. Series 537; American Chemical Society: Washington DC, 1993; p 370. (e) Renak, M. L.; Bazan, G. C.; Roitman, D. *Adv. Mater.* **1997**, *9*, 392. (f) Abdou, M. S. A.; Diaz-Guijada, G. A.; Arroyo, M. I.; Holdcroft, S. *Chem. Mater.* **1991**, *3*, 1003. (g) Perrson, S. H. M.; Dyreklev, P.; Inganäs, O. *Adv. Mater.* **1996**, *8*, 405. (h) Angelopoulos, M.; Shaw, J. M.; Lee, K.-L.; Huang, W.-S.; Lecorre, M.-A.; Tissier, M. *Polym. Eng. Sci.* **1992**, *32*, 1535. (i) Dai, L.; Mau, A. W. H.; Griesser, H. J.; Winkler, D.; Spurling, T.; Hong, X.; Yang, Y.; White, J. W. *Macromolecules* **1996**, *29*, 282. (j) Burn, P. L.; Holmes, A. B.; Kraft, A.; Bradley, D. D. C.; Brown, A. R.; Friend, R. H.; Gymer, R. W. *Nature* **1992**, *356*, 47. (k) Burn, P. L.; Kraft, A.; Baigent, D. R.; Bradley, D. D. C.; Brown, A. R.; Friend, R. H.; Gymer, R. W.; Holmes, A. B.; Jackson, R. W. *J. Am. Chem. Soc.* **1993**, *115*, 10117.

(10) (a) Dai, L.; Mau, A. W. H.; Gong, X.; Griesser, H. J. *Synth. Met.* **1997**, *85*, 1379. (b) Dai, L.; Griesser, H. J.; Mau, A. W. H. *J. Phys. Chem. B* **1997**, *101*, 9548.

(11) (a) Hwang, D. H.; Chuah, B. S.; Li, X.-C.; Kim, S. T.; Moratti, S. C.; Holmes, A. B. *Macromol. Symp.* **1997**, *125*, 111. (b) Chuah, B. S.; Hwang, D. H.; Kim, S. T.; Moratti, S. C.; Holmes, A. B.; deMello, J. C.; Friend, R. H. *Synth. Met.* **1997**, *91*, 279.

(12) (a) Gilch, H. G.; Wheelwright, W. L. *J. Polym. Sci.: A-1* **1966**, *4*, 1337. (b) Wessling, R. A. *J. Polym. Sci.: Polym. Symp.* **1985**, *72*, 55.

(13) Demas, J. N.; Crosby, G. A. *J. Phys. Chem.* **1971**, *75*, 991.

(14) Morra, M.; Occhiello, E.; Garbassi, F. *Adv. Coll. Interface Sci.* **1990**, *32*, 79.

(15) See, for example: *Organicum, Practical Handbook of Organic Chemistry*, Engl. transl.; Pergamon Press Ltd: Oxford, 1973.

Scheme 2

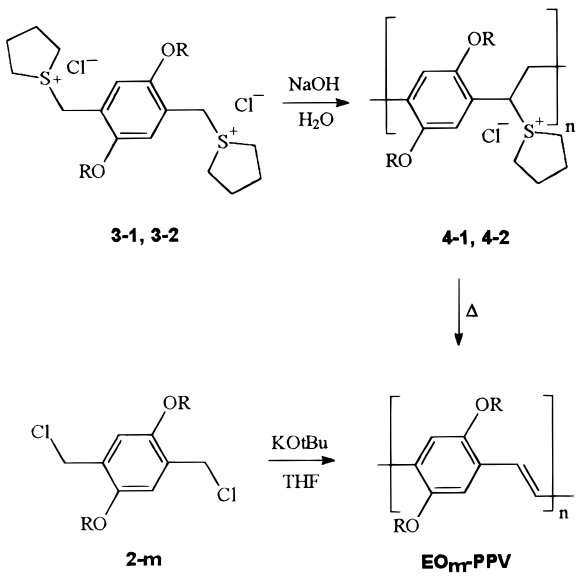

sulfonate (20.1 g, 87 mmol) and the mixture was further stirred at 60 °C for 2 days. After dilution with CH_2Cl_2, the organic layer was washed with NaOH (1 M), HCl (1 M), and water, respectively, yielding a yellow liquid of **1**−**1** (8.6 g, 38 mmol, 95%), which was used for the subsequent synthesis and characterization without further purification. ^{1}H NMR ($CDCl_3$): δ 6.85 (4H, phenyl, s), 4.06 (4H, PhOC*H*$_2$, t), 3.72 (4H, C*H*$_2$OCH$_3$, t), 3.44 (6H, OCH$_3$, s). ^{13}C NMR ($CDCl_3$): δ 152.6, 115.5, 71.1, 67.8, 59.1. IR (KRS-5, cm^{-1}): 3046, 2927, 2881, 2820, 1592, 1508, 1455, 1370, 1283, 1233, 1198, 1129, 1066, 1034, 926, 838, 755, 662, 532. Anal. Calcd for $C_{12}H_{18}O_4$: C, 63.66; H, 7.96; O, 28.29. Found: C, 63.67; H, 8.17; O, 28.53.

1,4-Bis(1,4,7-trioxaoctyl)benzene (1−2). The synthesis of **1**−**2** was similar to that for **1**−**1**, but EtOH was used as the solvent and KOH as the base. The reaction mixture was purified by silica gel chromatography using a mixture solvent of toluene and ethyl acetate to obtain the pale-yellow liquid, **1**−**2** (56%). ^{1}H NMR ($CDCl_3$): δ 6.80 (4H, phenyl, s), 4.05 (4H, PhOC*H*$_2$, t), 3.79−3.54 (12H, CH$_2$O, m), 3.35 (6H, OCH$_3$, s). ^{13}C NMR ($CDCl_3$): δ 153.0, 115.5, 71.9, 70.6, 69.8, 67.9, 59.0. IR (KRS-5, cm^{-1}): 3047, 2923, 2879, 2825, 1596, 1506, 1455, 1367, 1292, 1233, 1198, 1174, 1065, 931, 845, 756, 735, 704, 660, 554, 524.

1,4-Bis(1,4,7,10-tetraoxaundecyl)benzene (1−3). The synthesis of **1**−**3** was similar to that for **1**−**2**. Column chromatography led to a recovery of the pale-yellow liquid product at a yield of 43%. ^{1}H NMR ($CDCl_3$): δ 6.79 (4H, phenyl, s), 4.03 (4H, PhOC*H*$_2$, t), 3.75−3.60 (20H, CH$_2$O, m), 3.34 (6H, OCH$_3$, s). ^{13}C NMR ($CDCl_3$): δ 153.0, 115.5, 71.9, 70.7, 70.6, 70.5, 69.8, 68.0, 59.0. IR (KRS-5, cm^{-1}): 3045, 2919, 2871, 2828, 1593, 1507, 1456, 1359, 1291, 1229, 1121, 1067, 937, 840, 748, 659, 553, 525.

2,5-Bis(chloromethyl)-1,4-bis(1,4-dioxapentyl)benzene (2−1). The preparation of **2**−**1** was carried out according to a published procedure.[16] Briefly, a predetermined amount of **1**−**1** (2.6 g, 11.5 mmol) was added into a mixture of 1,4-dioxane (10 mL), concentrated HCl (37%, 10 mL), and aqueous formalin (37%, 5 mL) at 0 °C. Anhydrous HCl was bubbled through the reaction mixture for 30 min while the solution warmed to room temperature with stirring. After further stirring at room temperature for about 1 h, another 4 mL of formalin was then added at 0 °C and HCl gas was bubbled through the reaction mixture for 10 min. The above procedure was repeated, and the reaction mixture was then stirred overnight at room temperature. Thereafter, the reaction mixture was heated to reflux for 4 h. After cooling to room temperature, the solvents were completely removed to give a colorless solid residue. The solid material was then dissolved in a minimum amount of warm hexane. The hexane solution was poured into water and extracted with CH_2Cl_2 to produce a concentrated white residue, from which colorless crystals of **2**−**1** were obtained by crystallization from ethyl acetate at a yield of 30%. ^{1}H NMR ($CDCl_3$): δ 6.94 (2H, phenyl, s), 4.63 (4H, PhC*H*$_2$Cl, s), 4.13 (4H, PhOC*H*$_2$, t), 3.73 (4H, CH$_2$O, t), 3.44 (6H, OCH$_3$, s). ^{13}C NMR ($CDCl_3$): δ 150.7, 127.6, 115.1, 71.0, 69.0, 59.1, 41.1. IR (KRS-5, cm^{-1}): 3046, 2993, 2927, 2874, 1516, 1443, 1415, 1313, 1263, 1229, 1191, 1131, 1061, 1035, 958, 877, 856, 733, 701, 607.

2,5-Bis(chloromethyl)-1,4-bis(1,4,7-trioxaoctyl)benzene (2−2). **2**−**2** was prepared in a similar manner as **2**−**1**. Purification by silica gel chromatography using a mixed solvent of toluene and ethyl acetate led to the pale-yellow crystals of **2**−**2** (38%). ^{1}H NMR ($CDCl_3$): δ 6.94 (2H, phenyl, s), 4.63 (4H, PhC*H*$_2$Cl, s), 4.16 (4H, PhOC*H*$_2$, t), 3.86 (4H, PhOCH$_2$C*H*$_2$O, t), 3.72 and 3.56 (8H, CH$_2$O, 2t), 3.39 (6H, OCH$_3$, s). ^{13}C NMR ($CDCl_3$): δ 150.6, 127.5, 115.0, 72.0, 70.8, 69.7, 69.1, 59.1, 41.2. IR (KRS-5, cm^{-1}): 3043, 2925, 2876, 2824, 1509, 1450, 1415, 1355, 1314, 1217, 1125, 1060, 951, 855, 739, 702, 630.

2,5-Bis(chloromethyl)-1,4-bis(1,4,7,10-tetraoxaundecyl)benzene (2−3). **2**−**3** was prepared in a similar manner as **2**−**1**. Silica gel chromatography using a solvent mixture of toluene and ethyl acetate produced a yellow oil of **2**−**3** (20%). ^{1}H NMR ($CDCl_3$): δ 6.93 (2H, phenyl, s), 4.62 (4H, PhC*H*$_2$Cl, s), 4.14 (4H, PhOC*H*$_2$, t), 3.84 (4H, PhOCH$_2$C*H*$_2$O, t), 3.72−3.64 (16H, CH$_2$O, m), 3.36 (6H, OCH$_3$, s). ^{13}C NMR ($CDCl_3$): δ 150.5, 127.5, 115.0, 71.9, 70.8, 70.6, 70.5, 69.7, 69.1, 59.0, 41.1. IR (KRS-5, cm^{-1}): 3047, 2927, 2875, 2825, 1509, 1452, 1415, 1354, 1217, 1122, 1061, 951, 855, 738, 701, 630.

1,4-Bis(1,4-dioxapentyl)-2,5-bis(tetramethylenesulfonium)benzene dichloride (3−1). A certain amount of **2**−**1** (1.7 g, 5.26 mmol) and tetrahydrothiophene (1.5 mL, 17 mmol) in MeOH (20 mL) were stirred at 60 °C for 24 h. The reaction solution was then concentrated and slowly dropped into cold acetone. Reprecipitating in MeOH/acetone yielded the colorless salt of **3**−**1** (1.74 g, 3.44 mmol, 67%). ^{1}H NMR (D_2O): δ 7.25 (2H, phenyl, s), 4.57 (4H, PhC*H*$_2$S, s), 4.29 (4H, PhOC*H*$_2$, t), 3.91 (4H, C*H*$_2$OCH$_3$, t), 3.54 (8H, CH$_2$S, m), 3.38 (6H, OCH$_3$, s), 2.36 (8H, C*H*$_2$CH$_2$S, m). ^{13}C NMR (D_2O): δ 154.0, 123.0, 119.5, 73.8, 71.0, 61.2, 45.9, 43.6, 31.1. IR (KRS-5, cm^{-1}): 3008, 2950, 2897, 2814, 1513, 1465, 1401, 1310, 1232, 1127, 1051, 969, 918, 715. Anal. Calcd for $C_{22}H_{36}O_4Cl_2S_2$: C, 52.80; H, 7.20; O, 12.80; Cl, 14.18; S, 12.82. Found: C, 51.00; H, 7.31; O, 13.03; Cl, 15.53; S, 12.27.

1,4-Bis(1,4,7-trioxaoctyl)-2,5-bis(tetramethylenesulfonium)benzene dichloride (3−2). **3**−**2** was prepared in the same manner as **3**−**1**, but with a higher yield of 75%. ^{1}H NMR (D_2O): δ 7.31 (2H, phenyl, s), 4.59 (4H, PhC*H*$_2$S, s), 4.30 (4H, PhOC*H*$_2$, t), 3.97, 3.80 and 3.67 (12H, CH$_2$O, 3t), 3.54 (8H, CH$_2$S, m), 3.40 (6H, OCH$_3$, s), 2.38 (8H, C*H*$_2$CH$_2$S, m). ^{13}C NMR (D_2O): δ 154.0, 122.4, 119.4, 73.9, 72.4, 71.9, 71.0, 60.9, 45.9, 44.2, 31.2. IR (KRS-5, cm^{-1}): 3014, 2942, 284, 2829, 1512, 1458, 1436, 1399, 1312, 1234, 1136, 1111, 1057, 958, 849, 709. Anal. Calcd for $C_{26}H_{44}O_6Cl_2S_2$: C, 49.76; H, 7.02; O, 15.31; Cl, 11.31; S, 10.23. Found: C, 49.76; H, 7.88; O, 15.44; Cl, 11.79; S, 10.00.

Poly[1,4-(2,5-bis(1,4-dioxapentyl))phenylene-1-(tetramethylenesulfonium)-ethyl-1,2-ene chloride] (4−1). A predetermined amount of **3**−**1** (340 mg, 0.68 mmol) was dissolved in 20 mL of water under N_2. An equimolar amount of NaOH in water (0.5 mL) was slowly added into the ice-cooled, rapidly stirred aqueous solution of **3**−**1**, followed by further stirring for 1.5 h at ca. 5 °C. The polymerization reaction was then terminated by neutralization with an aqueous solution of HCl (1M). The resulting viscous, colorless polyelectrolyte solution of **4**−**1** was dialyzed against deionized water for 4 days at 4 °C to remove low molecular weight oligomers and unreacted monomers using a dialysis tube with a cutoff molecular weight of 6000 g/mol. IR (KRS-5, cm^{-1}): 3054, 2977, 2926, 2882, 2818, 1502, 1453, 1400, 1415, 1366, 1230, 1206, 1125, 1062, 941, 873, 678. A similar procedure was adopted to obtain **4**−**2**.

(16) Wudl, F.; Srdanov, G. U.S. Patent No. 5,189,136, 1993.

Poly[1,4-(2,5-bis(1,4,7,10-tetraoxaundecyl))phenylene vinylene] (EO_3−PPV). A solution of KO^{t}Bu (153 mg, 1.3 mmol) in dry THF (3 mL) was dropped into a rapidly stirred solution of **2**−**3** (0.59 g, 1.2 mmol, in 50 mL dry THF) under N_2. After having stirred the reaction mixture for 1 h at room temperature, additional dry THF (150 mL) and KO^{t}Bu (0.8 g, 7 mmol, in 5 mL dry THF) were added consecutively, and the reaction mixture was further stirred overnight. The resultant dark-red solution was slowly dropped into MeOH (400 mL) to produce the red polymer precipitate, from which 300 mg of EO_3−PPV (58%) was obtained by reprecipitation from CH_2Cl_2−MeOH. ^{1}H NMR ($CDCl_3$): δ 7.38 (2H, phenylene, m), 7.10 (2H, vinylene, m), 4.18 (4H, PhOCH_2, m), 3.85−3.35 (20H, CH_2O, m), 3.28 (6H, OCH_3, s). ^{13}C NMR ($CDCl_3$): δ 151.1, 127.6, 123.4, 111.1, 71.8, 70.9, 70.6, 70.5, 69.9, 69.2, 58.9. IR (free-standing film, cm^{-1}): 3060, 2926, 2876, 1504, 1455, 1421, 1354, 1251, 1206, 1121, 1069, 962, 855, 707. Anal. Calcd for $C_{22}H_{34}O_8$: C, 52.91; H, 6.81; O, 25.65. Found: C, 52.94; H, 6.17; O, 25.46.

LED Fabrication. Prior to construction of the LED devices, all the polymer solutions were filtered through a 0.45 μm Teflon membrane to remove insoluble particles. Single layer LEDs were then fabricated by spin coating a 2% solution of the soluble conjugated polymer in $CHCl_3$ or precursor polymer in H_2O/MeOH onto ITO glass and drying in a vacuum. In the case of the precursor polymer, the transformation to the conjugated structure was performed by heating in a vacuum (210−230 °C, 0.2−0.3 mTorr) for 4−5 h. Thereafter, the top contact was formed by thermal evaporation of aluminum onto either the preformed or the precursor-generated conjugated polymer layer.

Plasma Patterning. The equipment used for the plasma polymerization and the general procedure for plasma patterning have been previously described.[10b] In particular, plasma polymerization of acetic acid on FEP tapes (Du Pont FEP 100 Type A, 12.7 mm wide, 25 μm thick) and quartz substrates was carried out in a custom-built reactor, equipped with a disk-shaped lower electrode (95 mm in diameter) and a top electrode bar, which was powered by a commercial radio frequency generator (ENI HPG-2). Plasma pattern formation was achieved by using TEM grids as the mask.[10b] Substrates were purified through ultrasonication in $CHCl_3$ and EtOH, respectively, and dried by a N_2 stream. Both the patterned and nonpatterned plasma polymerizations were carried out at 125 kHz using a power of 10 W and a monomer pressure of 0.2 Torr for 30 s. Adsorption of the conjugated polymers in this study was achieved by immersing the freshly prepared plasma polymer surfaces in a solution of EO_3−PPV (2% in $CHCl_3$) for 20−30 min, followed by thoroughly rinsing them with dry chloroform. Prior to any physical characterization, the EO_3−PPV adsorbed plasma samples were dried by a N_2 stream and stored in clean polystyrene Petri dishes under N_2.

Results and Discussion

Polymer Synthesis. As outlined in Scheme 1, the methoxy-terminated oligo(ethylene oxide) chains were attached to a benzene ring in the para-position via Williamson ether formation between the corresponding alkoxy-*p*-toluenesulfonates and hydroquinone. Chloromethylation of the aromatic ethers with HCl in the presence of formaldehyde led to the bis-chloromethylated compounds **2-*m***. By reacting with tetrahydrothiophene (Scheme 1), **2**−**1** and **2**−**2** were transformed into the bis-sulfonium salts **3**−**1** and **3**−**2** for the preparation of the nonconjugated polyelectrolytes **4**−**1** and **4**−**2** (Scheme 2). As mentioned earlier, heating the polyelectrolytes **4**−**1** and **4**−**2** in a vacuum produced the corresponding conjugated polymers (EO_m−PPV, m = 1, 2) via the sulfonium precursor route. On the other hand, **2**−**3** was used *as synthesized* for the preparation of EO_3−PPV via the Gilch route (Scheme 2), as the product can dissolve well in THF.

In both cases, the high reactivity of the activated methylene groups (XH_2CPhCH_2X, X = halogen, SR_2, etc.) in the para-position leads to a very reactive quinoid intermediate after 1,6-elimination of HX in the presence of a base. This intermediate then undergoes radical and/or ionic 1,6-polymerization to produce an X-containing nonconjugated polymer, which can be transformed into the final conjugated polymer through 1,2-elimination of HX catalyzed by an excess amount of base, heating, or high-energy radiation.

Our attempts to produce soluble EO_1−PPV and EO_2−PPV from **2**−**1** and **2**−**2** via the Gilch route had little success, leading to either microgels/red precipitates during polymerization or a high content of insoluble material once being precipitated from methanol. A literature survey revealed that the above problem has been previously known and several modifications to the Gilch route have been made in order to circumvent it.[17,18] As an alternative approach, therefore, we have carried out the Gilch polymerization by first adding an equimolar amount of base into the reaction system. About 1 h later, the resultant orange solution was diluted with dry THF, to which an excess amount of the strong organic base was then added slowly. However, this approach was effective only for the monomer **2**−**3**, because the polymerization of monomers **2**−**1** and **2**−**2** was still complicated by the concomitant formation of insoluble materials, even in the highly diluted solution. Obviously, therefore, the interaction of the relatively short oligo(ethylene oxide) side chains in EO_m−PPVs (m = 1, 2) with THF is not strong enough to solubilize their conjugated backbones. As a consequence, we have chosen the sulfonium precursor route for preparing polymers EO_1−PPV and EO_2−PPV.

Spectroscopic Studies. NMR, FTIR, and MS spectroscopic measurements confirm the proposed chemical structures for all reaction products. In particular, ^{1}H NMR spectra for the symmetrically 1,2,4,5-substituted compounds **2-*m*** show singlets at ca. 6.94 ppm characteristic of the aromatic protons in the para-position. As depicted in Figure 1a, the ^{1}H NMR spectrum of EO_3−PPV shows the typical resonance of trans-substituted vinylene moieties at 7.1 ppm, while no signal is observable for its cis-counterpart in the region at around 6.5 ppm. The remaining proton resonances are attributed to the aromatic moiety (7.4 ppm), the ethyleneoxy groups (3.4−4.2 ppm), and the terminal methoxy group (3.3 ppm). The corresponding ^{13}C NMR spectrum given in Figure 1b shows three signals of the aromatic carbons at 111.1 (C-3), 127.6 (C-1), and 151.1 (C-2) ppm, together with the resonances of the olefinic C-atoms at 123.4 ppm and signals of the aliphatic carbons in the ethyleneoxy units over 69.2−71.8 ppm and the methoxy at 58.9 ppm.

The thermal transformation from **4-*m*** to EO_m−PPV (m = 1, 2, Scheme 2) was followed by FTIR and XPS. The FTIR spectra of the precursor polymer **4**−**1** before and after the thermal treatment are given in Figure 2 (traces a and b, respectively). In addition to the aromatic and the aliphatic (C−H) stretching modes between 2800 and 3010 cm^{-1}, Figure 2a shows strong (C−O) valence

(17) Hsieh, B. R.; Yu, Y.; VanLaeken, A. C.; Lee, H. *Macromolecules* **1997**, *30*, 8094.
(18) Hsieh, B. R.; Wan, W. C.; Yu, Y.; Gao, Y.; Goodwin, T. E.; Gonzales, S. A.; Feld, W. A. *Macromolecules* **1998**, *31*, 631.

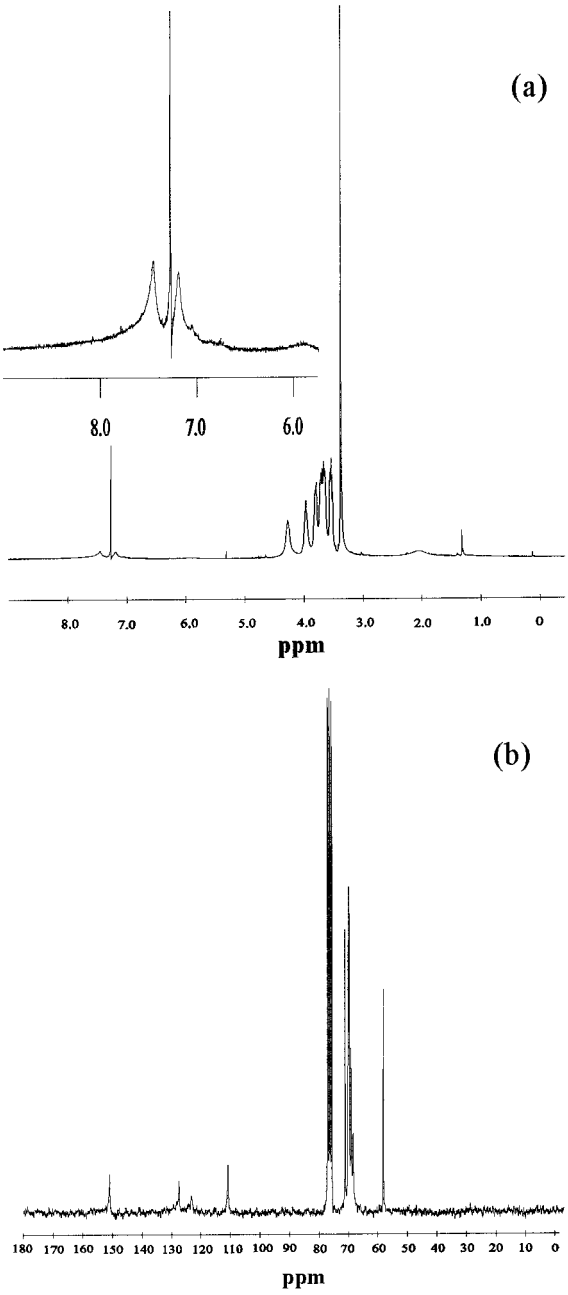

Figure 1. (a) ^{1}H and (b) ^{13}C NMR spectra of the polymer EO_3−PPV in $CDCl_3$.

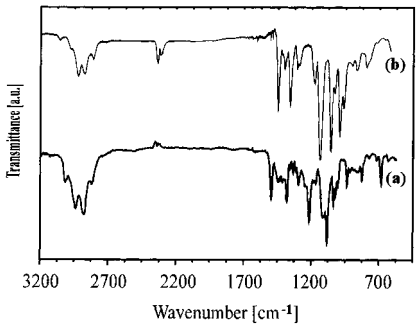

Figure 2. FTIR spectra of (a) precursor **4**−**1** and (b) fully converted EO_1−PPV.

modes of aromatic and aliphatic ethers (1050, 1130, 1300 cm^{-1}) and the typical (C═C) stretching modes of the aryl unit (1500 cm^{-1}) in the precursor polymer. As expected, Figure 2b shows the complete loss of the

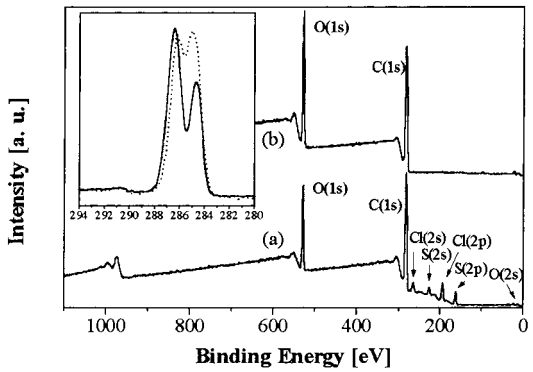

Figure 3. XPS survey spectra of (a) **4**−**1** and (b) EO_1−PPV. The inset shows the high-resolution C(1s) spectra of **4**−**1** (···) and EO_1−PPV (–).

characteristic (C−H) deformation vibration modes at 1230/1400 cm^{-1} and the (C−S) stretching mode at ca. 680 cm^{-1} of the tetrahydrothiophenium moiety. These spectroscopic changes are accompanied by the appearance of a new absorption band at 3060 cm^{-1} originating from the conjugated polymer main chain and a new peak at 990 cm^{-1} attributable to the out-of-plane (C−H) valence mode of trans-substituted vinylene groups. The high content of trans-configuration is also evidenced by the absence of the characteristic absorbance of cis-substituted alkene (ca. 730 cm^{-1}) in Figure 2b. Another significant feature shown in Figure 2 is the absence of any evidence for oxidation during the thermal conversion, which otherwise should be indicated by the carbonyl signals at 1650−1800 cm^{-1}. The FTIR spectra of **4**−**2**, EO_2−PPV, and EO_3−PPV are similar to those shown in Figure 2 but with subtle differences in intensities and maxima of absorption bands. The above spectroscopic results suggest a full conversion to the conjugated polymer backbone without any degradation of the side chains or polymer backbones under the experimental conditions used in this study.

Additional evidence for a full conversion from the polyelectrolyte precursor to the conjugated polymer comes from XPS measurements. Figure 3 shows the survey spectra of the freshly prepared polyelectrolyte **4**−**1** on quartz before (trace a) and after (trace b) the thermal conversion. As expected, Figure 3a shows the presence of C, O, Cl, and S in **4**−**1**. Figure 3b, however, gives no signal attributable to Cl or S. The corresponding high-resolution C(1s) spectra are shown in the inset of Figure 3. The large decrease in the aliphatic carbon peak (285 eV) associated with **4**−**1** upon the thermal treatment indicates the loss of the tetrahydrothiophene units. The C(1s) spectrum of EO_1−PPV does not show any signals for C═O or O−C═O between 288 and 289.5 eV, suggesting, once again, the absence of any oxidation products.[19] A shake-up band characteristic of the conjugated structure is visible over 290−292 eV. The atomic ratio of the ether carbons (ca. 286.6 eV) to carbons of the conjugated backbone (ca. 284.7 eV) is calculated to be 8:6, in good agreement with the structure of the monomer unit in EO_1−PPV.

Optoelectronic Properties. All EO_m−PPVs are red and show similar optical and PL spectra (Figure 4). The

(19) Xing, K. Z.; Johansson, N.; Beamson, G.; Clark, D. T.; Brédas, J.-L.; Salaneck, W. R *Adv. Mater.* **1997**, *13*, 1027.

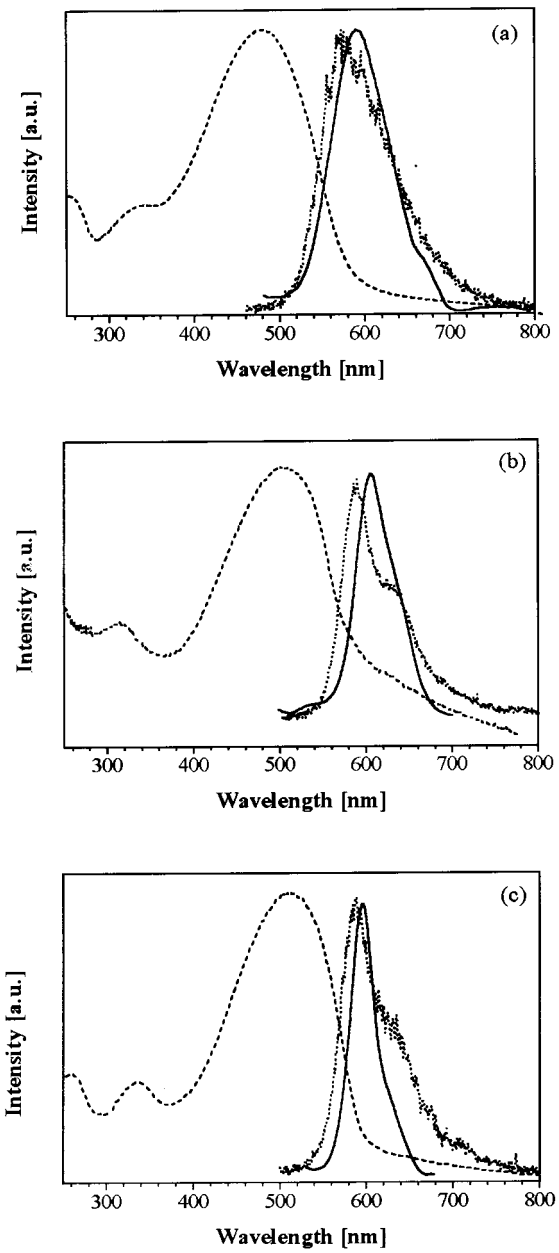

Figure 4. UV−vis absorbance (- -), PL (—) (λ_{ex} = 375 nm), and EL (···) spectra of EO_m−PPV, (a) m = 1, (b) m = 2, and (c) m = 3.

strong, broad optical absorbance over 400−600 nm can be attributed to the π−π* electron transition associated with the π-conjugated polymer backbones. The wavelength for the maximum optical absorbance shifts from 476 nm through 501 nm to 511 nm for m =1, 2, and 3, respectively, whereas there is almost no change in the band gap energy (2.14 eV for m = 1 and 2.13 eV for m = 2, 3), as indicated by the nearly identical absorption edges between 580 and 582 nm.

On the other hand, all EO_m−PPVs show strong orange-red PL emissions with a maximum at around 600 nm. It is of surprise to note that the room-temperature PL emission peaks are all very narrow (e.g., the full width at half-maximum (fwhm) is ca. 35 nm for EO_3−PPV, though its molecular weight distribution is as high as 2.7 and $\bar{M}_w$ = 2.2 × 10^5 g/mol). Although the molecular weights of the sulfonium precursor polymers for EO_1−PPV and EO_2−PPV are not

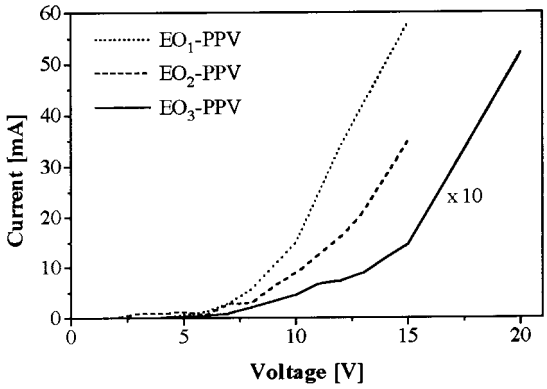

Figure 5. Current−voltage (I−V) characteristics of LEDs (ITO/EO_m−PPV/Al).

determined, they, most probably, are also higher than 10^5 g/mol, a minimum value of the $\bar{M}_w$ which has been reported for most precursor polymers from the sulfonium precursor route.[20] Therefore, the sharp emissions seen in Figure 4a−c presumably indicate a narrow distribution of the geometries and sites of the emitting molecular structures along the polymer backbones. The PL quantum efficiency of EO_3−PPV measured in a CH_3CN solution is relatively high (Φ = 0.55), although the corresponding value for a solid film is only about 10%, as is the case for certain other substituted PPVs.[6a,11b,21]

Single layer LEDs based on EO_m−PPV show EL emissions similar to the PL emission, but with a small hypsochromic shift. This indicates, as expected, the same singlet excitons being responsible for both the EL and PL emissions. As shown in Figure 5, the turn-on voltages for LEDs with the structure ITO/EO_m−PPV/Al are about 7 V (layer thickness is ca. 100 nm), whereas the current decreases significantly with the increase in m at a constant applied voltage. The observed constant turn-on voltages may indicate that the charge injection barriers between the electrodes and the EL polymers are, more or less, independent of the side chain length, as is the case for the band gap energy (vide supra). However, the reverse proportional relationship between the current and the length of the side chains suggests that the efficiency of charge transport in the conjugated polymer is reduced by the presence of oligo(ethylene oxide) side chains and that the longer side chains should lead to higher intermolecular electrical resistances. Nevertheless, this drawback may be overcome by making LECs from the EO_m−PPVs, in which the oligo(ethylene oxide) substituents can act as ionically conducting, rather than insulating, components in the presence of appropriate Li salt(s). Our preliminary results from LECs with the structure ITO/EO_m−PPV + CF_3SO_3Li/Al indicate a turn-on voltage as low as 2.2 V, along with the I−V characteristic being independent of the side chain length. It is worthwhile to point out that these LECs do not require additional poly(ethylene oxide) homopolymers for ionic conduction. The detailed fabri-

(20) (a) Lenz, R. W.; Han, C.-C.; Stenger-Smith, J.; Karasz, F. E. *J. Polym. Sci. A, Polym. Chem.* **1988**, *26*, 3241. (b) Köpping-Grem, G.; Leising, G.; Schimetta, M.; Stelzer, F.; Huber, A. *Synth. Met.* **1996**, *76*, 53.

(21) The solid PL efficiency was measured according to a published procedure and cross-checked with MEH−PPV (see, de Mello, J. C.; Wittmann, H. F.; Friend R. H. *Adv. Mater.* **1997**, *9*, 230).

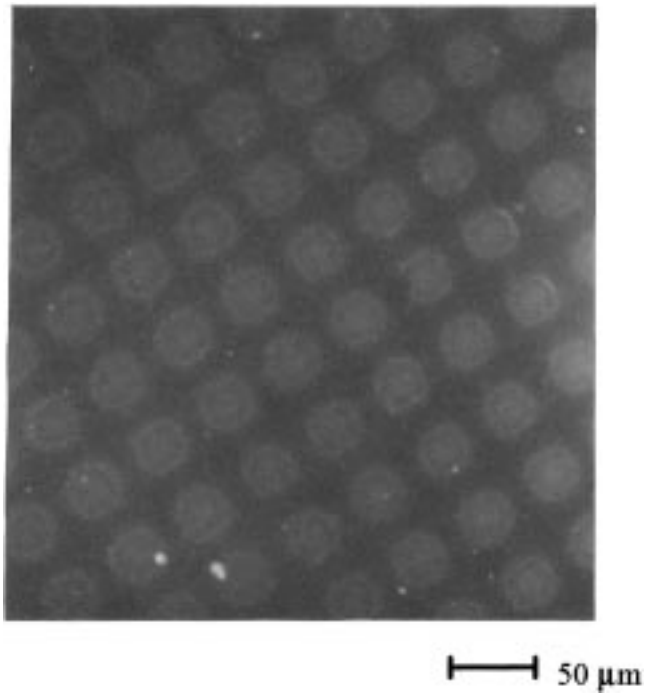

Figure 6. Fluorescent microscopic image of EO_3−PPV on plasma patterned FEP. The rather poor contrast seen in the image is due to the relatively weak fluorescence emission from a very thin layer of the adsorbed EO_3−PPV.

cation and performance evaluation of the LECs based on EO_m−PPVs are currently in progress and will be reported elsewhere.[22]

Plasma Patterning. On the basis of our previous work on plasma patterning,[10] we have developed a patterning technique for the EO_m−PPVs. We first prepared hydrophilic patterns by plasma polymerization of acetic acid on FEP or quartz substrates. The conjugated polymer patterns were then obtained by selective adsorption from a solution of EO_3−PPV in $CHCl_3$. As we shall see later, it is the polar−polar interaction between the oligo(ethylene oxide) side chains and the region specifically deposited with the polar plasma polymer that ensures the PPV derivative be selectively adsorbed on the plasma polymer layer. Although the plasma polymerization of acetic acid has been much less discussed in the literature with respect to other unsaturated hydrophilic monomers,[23] the acetic acid plasma polymer (AAPP) was found to have good mechanical and chemical stabilities (no detachment of the plasma polymer from the substrate was observed during storage in air or in the solvent), together with a strong interaction with poly(ethylene oxide) chains.[24] These unusual properties made acetic acid the monomer of choice.

Figure 6 shows a typical fluorescence microscopic image of the patterned EO_3−PPV on the plasma-treated FEP, which is a close replica of a TEM grid used as the mask.[10b] As can be seen, the plasma-treated regions gave fluorescence emissions characteristic of the adsorbed conjugated polymer, consistent with the polymer adsorption originating from the polar−polar interaction, as mentioned above. No adsorption of the EO_3−PPV was observed in a control experiment when pure FEP was used as the substrate. If a piece of the AAPP prepatterned *quartz* was used as the substrate, however, EO_3−PPV was found to adsorb throughout the substrate surface. At first sight, this seems to be inconsistent with the observation made on the plasma-patterned FEP, but we note that a clean quartz surface is more hydrophilic than the AAPP layer (Table 1). As can be seen from Table 1, the ACA = 122°, SCA = 112°, and RCA = 104° for untreated FEP were reduced to values of 66°, 54°, and 21°, respectively, by the acetic acid plasma treatment. In contrast, the same plasma treatment on a quartz surface caused an increase in the air/water contact angles. We found that different cleaning procedures could lead to different contact angles for the cleaned quartz surfaces.[25] Although we can make a quartz substrate with very low contact angles (see, quartz[b] in Table 1) through a rather tedious cleaning procedure, we used the same cleaning method for both the FEP and quartz substrates in this study (see, FEP[a] and quartz[a] in Table 1). Clearly, therefore, it is the similarity in the surface hydrophilicity, and hence polarity, between the untreated and the plasma-treated quartz surface (i.e., quartz[a] and quartz/AAPP in Table 1) that is responsible for the nonselective adsorption of EO_3−PPV in this particular case. Rather than being a contradiction, therefore, the results obtained from the quartz substrate further indicate that the strong polar interaction indeed is the driving force for patterning EO_3−PPV onto the AAPP surfaces. Furthermore, the very similar air/water contact angles between a spin-cast film of EO_3−PPV (i.e., EO_3−PPV[c] in Table 1) and the polymer adsorbed layers on the plasma treated surfaces (i.e., FEP/AAPP/EO_3−PPV and quartz/AAPP/EO_3−PPV in Table 1) indicate that EO_3−PPV cannot only specifically adsorb onto the AAPP prepatterned surfaces with a micrometer precision but also form a pinhole-free, homogeneous thin film necessary for EL applications. This simple method for the pattern formation of PL/EL-active polymers, therefore, could have potential implications for making patterned light emission units of use in various electronic and photonic devices.

Table 1. Advanced (ACA), Sessile (SCA), and Receding (RCA) Contact Angles

sample	ACA (deg)	SCA (deg)	RCA (deg)
FEP[a]	122	112	104
FEP/AAPP	66	54	21
FEP/AAPP/EO_3−PPV	59	46	14
quartz[a]	49	30	10
quartz[b]	16	11	<10
quartz/AAPP	63	57	21
quartz/AAPP/EO_3−PPV	58	48	12
EO_3−PPV[c]	62	45	12

[a] Purified with $CHCl_3$ and EtOH. [b] Purified with concentrated HCl, Caro's acid, and Milli-Q water. [c] Spin coated on quartz.

(22) (a) Tasch, S.; Holzer, L.; Wenzl, F. P.; Gao, J.; Winkler, B.; Dai, L.; Mau, A. W. H.; Sotgiu, R.; Sampietro, M.; Leising, G.; Heeger, A. J. *Synth. Met.* **1998**, accepted. (b) Holzer, L.; Tasch, S.; Winkler, B.; Dai, L.; Mau, A. W. H.; Leising, G. *Adv. Mater.*, to be published.

(23) See, for example: (a) O'Toole, L.; Beck, A. J.; Ameen, A. P.; Frank, F. R.; Short, R. D. *J. Chem. Soc.* Faraday Trans. 1995, *91*, 3907. (b) O'Toole, L.; Beck, A. J.; Short, R. D. *Macromolecules* **1996**, *29*, 5172. (c) Yasuda, H. *Plasma Polymerization*; Academic Press: Orlando, FL, 1995.

(24) Gong, X., private communication.

(25) Scales, P. J.; Grieser, F.; Furlong, D. N.; Healy, T. W. *Colloids Surf.* **1986**, *21*, 55.

Conclusions

We have prepared various poly(*p*-phenylene vinylene)s disubstituted with oligo(ethylene oxide)s (EO_m−PPV, EO_m = $CH_3O(CH_2CH_2O)_m$ and m = 1−3) and demonstrated the influence of the side chain length on optoelectronic properties. While the sulfonium precusor route was chosen for making the polymers with short side chains (m = 1 and 2), a modified Gilch route was applied for the preparation of EO_3−PPV. The conjugated EO_m−PPVs (m = 1−3) thus prepared have constant band gap energies (Eg) of ca. 2.14 eV and show similar orange-red emissions with $\lambda_{max} \approx 600$ nm upon both photo- and electroexcitation. However, the $I-V$ characteristics of LEDs based on them are strongly influenced by the length of the polar substituents. Patterning of EO_3−PPV on FEP films prepatterned with acetic acid plasma was achieved simply by immersing the plasma-treated substrate into the polymer solution. The strong polar−polar interaction between the oligo(ethylene oxide) side chains of the conjugated polymer and the polar plasma polymer surface is shown to be responsible for the fluorescent pattern formation. This work presents new materials and patterning technology of potential applications in optoelectronic devices.

Acknowledgment. B.W. thanks the Austrian Science Fund, Vienna, for providing him an Erwin-Schrödinger-Auslandsstipendium (FWF Project J1426-CHE). We would also like to thank Drs. X. Gong, Limin Dong, and Mr. G. Georgaklis for assistance in plasma treatment, solid PL efficiency measurement, and fluorescent microscopy, respectively.

CM980570M